



# Trend analysis of extreme rainfall indices from CHIRPS precipitation estimates over the Lake Tana sub-basin, Abbay Basin of Ethiopia

Jemal Ali Mohammed

Received: 6 December 2023 / Accepted: 13 May 2024 / Published online: 24 May 2024  
© The Author(s), under exclusive licence to Springer Nature Switzerland AG 2024

**Abstract** Ethiopia is among the African nations most susceptible to climate change because of its frequent droughts and heavy rainfall. Therefore, hydrological and water management problems require an investigation of regional variability and extreme rainfall patterns. This study analyzed the spatiotemporal trends of extreme rainfall in the Lake Tana sub-basin (LTSB) of Ethiopia's upper Blue Nile basin (UBNB) between 1981 and 2019. The trend and geographic patterns of ten extreme rainfall indices are evaluated using high-resolution data from Climate Hazards Group InfraRed Precipitation Stations (CHIRPS). The researcher used RClimDex, an R software tool, to analyze the ten severe rainfall indices. The variability of the extreme rain indices was also assessed by applying the standard anomaly index (SAI). The trend analysis shows that the majority of rainfall indices decreased in the majority of station locations. Among the rainfall locations, the decreasing trend was only significant in 40% consecutive wet days (CWD), 13.33% (R95p and R99p), and 6.66% highest rainfall amount in a 1-day period (RX1day). In contrast, significant positive patterns were revealed in the incidence of rainfall events of number of heavy precipitation days (R10mm), annual total wet day rainfall

(PRCPTOT), and consecutive dry days (CDD), with significant positive trends of 26.66% (R10mm) and 40% (PRCPTOT). Furthermore, a spatial distribution result of extreme rainfall trends reveals considerable variations between stations location. Thus, these findings point to the necessity of creating adaptation and mitigation plans for climate change variability within the sub-basin.

**Keywords** Climate sciences · CHIRPS estimates · Climatic indices · ETCCDI · Rainfall variability · Climate adaptation

## Introduction

Weather or climate extreme occurs when a variable's value exceeds or falls beyond an ideal value far from the observed range of the variable's value (IPCC, 2012). Climate change is related to rising concentrations of greenhouse gases in the environment, which have amplified the world's mean annual temperature of the surface by 0.07 °C per decade since 1880 (IPCC, 2013, 2018). Almost all seasons worldwide have experienced an upward in temperature trends in recent years (Cohen et al., 2012; Rossati, 2017). Global climate change has made extreme precipitation events a hot issue in recent years, and their frequency and intensity are on the rise (IPCC, 2012; Pendergrass et al., 2017; IPCC, 2013, 2021). Based on a study by Donat et al. (2016), most portions of the

J. A. Mohammed (✉)  
Department of Forestry, College of Agriculture  
and Natural Resources, Mekdela Amba University,  
Tulu Awlya, Ethiopia  
e-mail: Jemalali344@gmail.com; mjemalali11@gmail.com

earth experience positive trends in extreme rainfall events. Extreme rainfall trends are far less regionally homogenous than changing temperature trends (Alexander et al., 2006). Research from India, Europe, Ethiopia, the United States, Canada, Ghana, and Eastern Africa, as well as the western drift of Northern America, confirms that severe rainfall events are distinct across regions (Agilan & Umamahesh, 2018; Bezerra et al., 2019; Cardell et al., 2020; Casanueva et al., 2014; Hagos et al., 2016; Mladjic et al., 2011; Mutiibwa et al., 2015; Wubaye et al., 2023).

Anthropogenic climate change is expected to continue changing global extreme rainfall characteristics (Westra et al., 2013; IPCC, 2021). Forecasts of excessive rainfall show seasonal changes and spatial variability over different areas of the world. The analysis of extreme rainfall is similar to historical studies. According to Almazroui et al. (2021), rainfall is predicted to decrease over Southern America, Chile, and Amazonia's southern Andes, while it is expected to rise over South America and the Pacific Ocean. Likewise, Almazroui et al. (2020) report a fallen rainfall in Africa's northern and southern regions, but rising in the central areas. Severe rainfall occurrences are more sensitive to the effects of climate change and represent greater hazards to the natural system than mean climatic values (IPCC, 2018).

Ethiopia is a climate extreme area due to its great regional and temporal variation in temperature as well as rainfall (Berhane et al., 2020; Gebrechorkos et al., 2019; Jothimani et al., 2020; Mengistu et al., 2013; Wubaye et al., 2023). In consequence, climate extremes have profound effects on local economies, environments, and populations. As a result, understanding and analyzing climate extremes is essential for reducing damage caused by climate extremes. This provides people with timely warnings so they can cope or adapt better (Asfaw et al., 2018; IPCC, 2013; Wubaye et al., 2023). In order to address this need, many studies (e.g., Ademe et al., 2020; Geremew et al., 2020; Gummadi et al., 2018; Weldegerima et al., 2018) have examined rainfall and temperature trends; however, fewer studies have investigated past trends and forecast extreme rainfall events. In the Jemma sub-basin, for example, Worku et al. (2019) evaluated changes in rainfall extremes and found that there were less spatially coherent positive trends. Nevertheless, there is a rise in precipitation and a decline in the number of dry days in various areas of Ethiopia (Gummadi et al., 2018; Teshome & Zhang,

2019; Worku et al., 2019; Wubaye et al., 2023). Ethiopia's results are generally in line with studies globally that show more complex, but generally wet rainfall extremes (Donat et al., 2016). However, extreme rainfall exhibits inconsistent trends because of high spatial and temporal variability (Dendir & Birhanu, 2022; Worku et al., 2019; Wubaye et al., 2023).

Most studies in Ethiopia are conducted on the whole country and large watersheds with different climates. In addition, the lack of adequate data limits the applicability of this method in the analysis of data at different locations in Ethiopia (Mohammed et al., 2022; Teshome & Zhang, 2019; Wubaye et al., 2023). Therefore, analyzing the regional and temporal patterns of precipitation extremes at the sub-area scale is imperative in order to put into practice suitable native adaptation and mitigation measures for climate extremes. The Lake Tana sub-basin of UBNB, which is prone to periodic droughts and intense rainfall (Bayissa et al., 2015; Mohammed et al., 2022), is the focus of this study. More than any other sub-basin of the upper Blue Nile basin (UBNB), the Lake Tana sub-basin (LTSB) is described by high levels of soil erosion and sedimentation. Thus, two recent phenomena that can serve as exemplary illustrations of uncommon events in the basin are the low water level of Lake Tana in 2003 and its dramatic rise in 2006 as a result of a flood disaster in the Fogera floodplain (Moges & Moges, 2019). This research assesses the temporal pattern and spatial variation of extreme rainfall by utilizing data from the Climate Hazard Group InfraRed Rainfalls with Stations (CHIRPS) satellite estimate over the LTSB. The results of this study would help future investigations into climate change. Additionally, a significant contribution from this research will fill in several gaps in the body of current knowledge. It will close the knowledge gap and expand on the scant research on the variability of extreme rainfall in a region often impacted by climate-related hazards. It is also expected to assist in the development of strategies for mitigation and adaptation to heavy rainfall events.

## Material and methods

### Study area description

The LTSB, belonging to the UBN (Abbay) basin's sub-basins, covers an estimated 15,096 km<sup>2</sup>, of which

Lake Tana occupies 3063 km<sup>2</sup>. Lake Tana is the largest lake in Ethiopia, spanning 3000–3600 km<sup>2</sup> and reaching a maximum depth of 15 m at 1800 m above sea level (m.a.s.l) (Chakilu et al., 2022). The LTSB is found in the north-western Ethiopian plateaus with latitudes of 10.95°N and 12.78°N, and longitude of 36.89°E and 38.25°E (Fig. 1). The basin's average altitude is 2025 m.a.s.l, having the highest peak of 4100 m.a.s.l located in the northeastern Semien Mountains (Wubneh et al., 2022).

In the basin, there is a tropical highland monsoon climate, attributed to a mono-modal rainfall pattern, with rainfall peaks occurring in June and September throughout the rainy season (Uhlenbrook et al., 2010). For the period 1976–2005, rainfall fell between 764.38 and 2340.94 mm (Wubneh et al., 2022). The distribution of rainfall in the area is regulated by inter-tropical convergence zones (ITCZ) (Uhlenbrook et al., 2010). The air temperature fluctuates a lot during the day, although it only slightly changes over the season, with an average annual temperature of 20 °C. Agro-pastoral land makes up 29% of the LTSB's land area, 20% of which is covered by lakes, while agriculture accounts for 51.3% of the basin's total land area (Setegn et al., 2008).

#### Source of climate data and quality control

There is a need for long-term and temporally homogeneous climate data for many different applications, such as climate risk management and climate change adaptation. One of the major limitations to using climate information in Ethiopia is the lack of reliable climate data (Dinku et al., 2014). Most climate data come from weather stations, which are irregularly located and mainly found along major routes in cities and towns (Alemu & Bawoke, 2020; Bayissa et al., 2017; Dinku et al., 2014). Moreover, rainfall data originating from meteorological stations were often incomplete and recorded over short periods. Many users in Ethiopia are compelled to rely on satellite rainfall predictions due to the unavailability of rain gauge observations (Alemu & Bawoke, 2020; Bayable et al., 2021; Dinku et al., 2018). I used the Climate Hazards Group Infrared Rainfall with Stations (CHIRP) high-resolution satellite data on rainfall for this work. The Climate Hazards Group at the University of California, Santa Barbara (UCSB) and the US Geological Survey (USGS) collaborated to produce

this daily-updated product (Funk et al., 2015). The researcher was drawn to this recently created satellite product because of its long-term rainfall data and comparatively excellent spatial resolution. Furthermore, it offers low-cost data on precipitation for various time periods.

Data on historical rainfall within the basin were provided by Ethiopia's National Metrological Agency (NMA). I obtained eight high-quality stations from the NMA, of which five were used to validate the CHIRPS satellite estimate (Table 1). A few stations were removed in the final analysis due to missing rainfall data (more than 10%). I used the Multivariate Imputation by Chained Equations (MICE) technique (Buuren, 2015) to fill in the missing data. Moreover, station data were subjected to quality control and homogeneity tests using Microsoft Excel and RCLindex (Zhang & Yang, 2004). To assess the CHIRPS satellite estimate product's performance, I converted the quality-controlled gauge measurements of daily data into annual and monthly data.

#### Validation of CHIRPS rainfall data

In drought and flooding-prone areas, accurate precipitation estimation is essential. Satellite weather data collection has become an alternative method for estimating precipitation due to advancements in remote sensing (RS) (Avtar et al., 2020; Bhaga et al., 2020). Currently, a variety of precipitation datasets is being used, including but not limited to CHIRPS, which is a ground-based and RS-based precipitation dataset. However, there are uncertainties that can result in significant errors in satellite-based rainfall patterns and variability assessments due to various sampling errors, algorithm errors, and satellite instruments (Bayable et al., 2021; Belay et al., 2019; Dinku et al., 2018; Fenta et al., 2018). Therefore, these gridded precipitation datasets should be evaluated and validated against in situ observations to guarantee data quality. (Dinku et al., 2014; Belay et al., 2019; Dembele and Zwart, 2016).

It was shown that the CHIRPS dataset is effective in African countries, including Ethiopia. Based on the findings of Dembele and Zwart, 2016, Bayissa et al., 2017 and Kimani et al., 2017, CHIRPS estimates outperform the majority of other long-term satellite rainfall datasets. Despite this, more studies and research on different parts of Ethiopia are

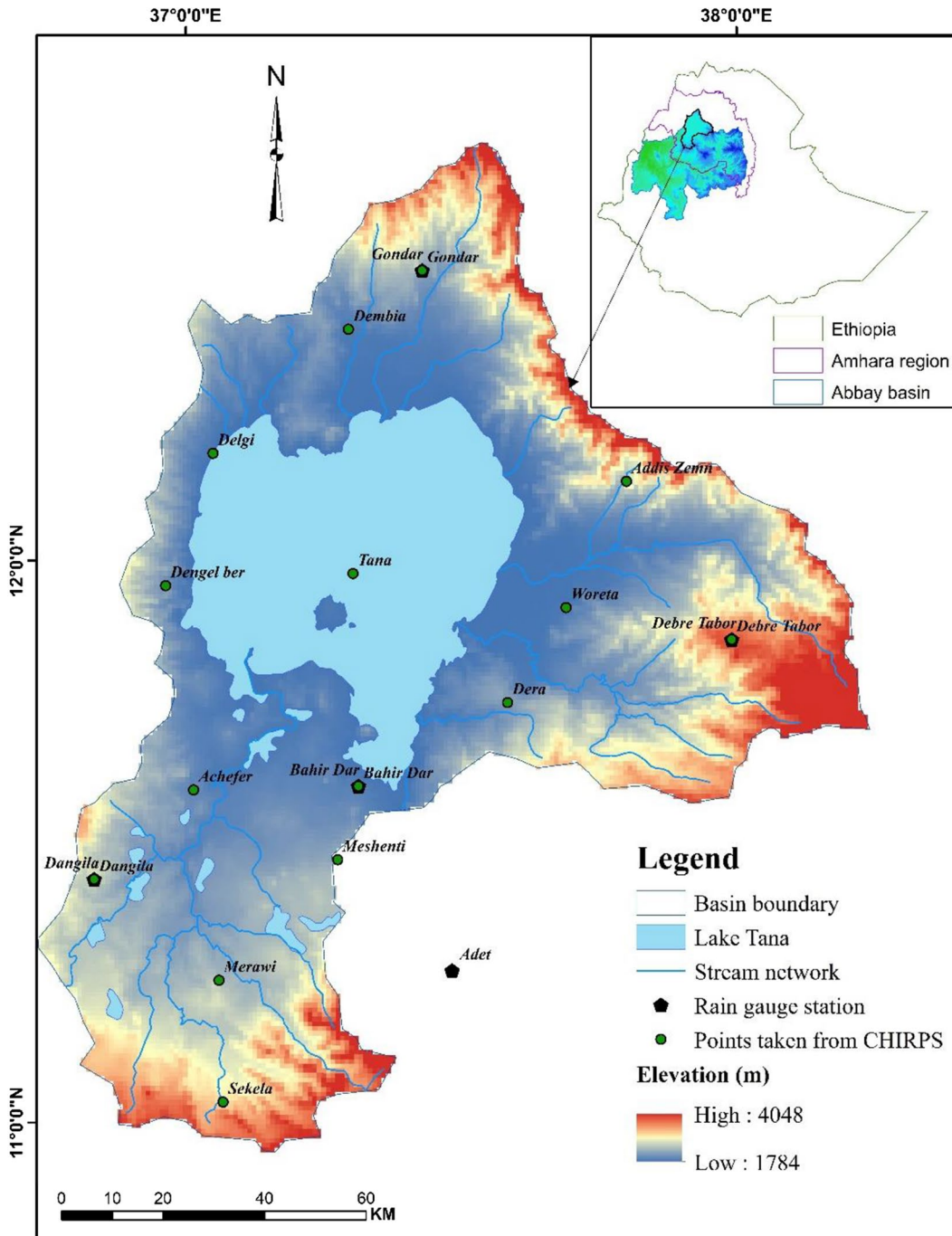


**Fig. 1** Location of LTSB from Ethiopia and the climatic stations that were utilized

needed on various geographical and temporal scales (Kimani et al., 2017). The researcher downloaded CHIRPS Rainfall predictions in raster form and then utilized Python 3.8.5 to get all required values for

points at a spatial resolution of 0.05° latitude-longitude (Rossum & Drake, 2001). By comparing the extracted point-oriented CHIRPS precipitation data from the LTSB regions (Table 2) with the data from

**Table 1** List of the rainfall gauges that were used to validate the CHIRPS rainfall estimate

No	Stations	Geographical coordinates		Elevation	Period of record	Missing data (%)
		Latitude (°)	Longitude (°)			
1	Adet	11.27	37.49	2179	1988–2019	4.5
2	Bahir Dar	11.61	37.32	1827	1988–2019	8.5
3	Gondar	12.52	37.43	1973	1980–2019	3.5
4	Dangila	11.43	36.84	2116	1987–2019	5.5
5	Debre Tabor	11.86	37.99	2612	1980–2019	7.5

the ground-oriented stations, the CHIRPS rainfall data were validated on monthly and yearly time periods. A number of statistical indicators, such as correlation coefficients (*r*), mean absolute error (MAE), root mean square error (RMSE), and Nash–Sutcliff coefficients (NSE) were employed to confirm that the CHIRPS data were suitable for additional analysis (Table 3). Validation statistics have been chosen based on other study selections in order to compare CHIRPS satellite rainfall predictions with data from rainfall gauge (e.g., Ayehu et al., 2018; Dinku et al., 2018; Kimani et al., 2017), with descriptions as below:

(i) The correlation coefficient (*r*) compares the similarities of average CHIRPS data to the observed data. The *r* values can range between 0.0 and 1.0, with higher values indicating better agreement and lower values indicating less agreement (Mohammed & Yimam, 2022). The correlation coefficient (*r*) was calculated using the formula:

$$r = \frac{\sum_{i=1}^n (M_i - \bar{M})(Z_i - \bar{Z})}{\sqrt{\sum_{i=1}^n (M_i - \bar{M})^2 \sum_{i=1}^n (Z_i - \bar{Z})^2}} \tag{1}$$

where *M<sub>i</sub>* is the observation value, *Z<sub>i</sub>* is the CHIRPS value, *M<sub>bar</sub>* is the average of reference values, and *Z<sub>bar</sub>* is the average of CHIRPS values.

(ii) The MAE gives information about the average estimation error from the ground-based observed data. The value of MAE ranges from 0 to 1, with a perfect score of 0. It was estimated using the following formula.

$$MAE = \frac{1}{n} \sum_{i=1}^n (M_i - Z_i) \tag{2}$$

where *M<sub>i</sub>* is the rain gauge value, and *Z<sub>i</sub>* is the CHIRPS rainfall value.

(iii) The NSE is defined as one minus the sum of the absolute squared differences between the CHIRPS

**Table 2** List of chosen CHIRPS points

No	Place of point	Location	Geographical coordinates		Elevation
			Latitude (°)	Longitude (°)	
1	Achefer	South-western	11.594	37.024	2445
2	Addis Zemn	North-eastern	12.148	37.804	2300
3	Bahir Dar	South-eastern	11.603	37.322	1827
4	Dangila	South-western	11.434	36.846	2116
5	Debre Tabor	Eastern	11.867	37.995	2612
6	Delgi	North-western	12.193	37.055	1661
7	Dembia	Northern central	12.416	37.299	2026
8	Dengel ber	North-western	11.957	36.971	1840
9	Dera	South-eastern	11.753	37.591	2455
10	Gondar	Northern	12.521	37.432	1973
11	Merawi	Southern central	11.256	37.073	2045
12	Meshenti	South-eastern	11.472	37.285	1944
13	Sekela	Southern	11.039	37.082	2915
14	Tana	Central	11.981	37.310	1780
15	Woreta	Northern central	11.922	37.696	1780

**Table 3** Description of the selected indices

Indices	Index name	Definition of the index	Unit
PRCPTOT	Annual total wet-day rainfall	Annual total PRCP in wet days ( $RR \geq 1$ mm)	mm
R99p	Rainfall on extremely wet days	Annual total PRCP when $RR > 99$ th percentile	mm
R95p	Rainfall on very wet days	Annual total PRCP when $RR > 95$ th percentile	mm
R20	Number of very heavy precipitation days	Annual count of days when $PRCP \geq 20$ mm	Days
R10	Number of heavy precipitation days	Annual count of days when $PRCP \geq 10$ mm	Days
CWD	Consecutive wet days	Maximum number of consecutive days with $RR \geq 1$ mm	Days
CDD	Consecutive dry days	Maximum number of consecutive days with $RR < 1$ mm	Days
SDII	Simple daily intensity index	Annual total precipitation divided by the number of wet days (defined as $PRCP \geq 1.0$ mm) in the year	mm/day
RX5day	Highest rainfall amount in a 5-day period	Monthly maximum consecutive 5-day precipitation	mm
RX1day	Highest rainfall amount in a 1-day period	Monthly maximum 1-day precipitation	mm

and the reference values normalized by the variance of the reference value during the evaluation period, with 1 being the perfect value. The NSE can have values ranging from  $-\infty$  to 1. The closer the result is to 1, the better the CHIRPS precipitation estimations are (Nash & Sutcliffe, 1970). It was computed using the formula:

$$NSE = 1 - \frac{\sum_{i=1}^n (M_i - Z_i)^2}{\sum_{i=1}^n (M_i - \bar{M})^2} \quad (3)$$

where  $M_i$  is the observation value,  $Z_i$  is the CHIRPS value,  $\bar{M}$  is the average of reference values, and  $\bar{Z}$  is the average of CHIRPS values.

(iv) RMSE calculates the difference between CHIRPS precipitation data and actual rainfall values. RMSE values vary from 0 to  $\infty$ , with a value near zero indicating greater performance (Mohammed & Yimam, 2022). It was calculated using the following equation:

$$RMSE = \frac{\sqrt{\sum_{i=1}^n (M_i - Z_i)^2}}{j} \quad (4)$$

where  $j$  is the length of the time series,  $M_i$  is the meteorological gauge rainfall value, and  $Z_i$  is the CHIRPS rainfall value

#### Spatial and temporal trend examination of rainfall indices

Using daily rainfall data to calculate climate indices is one way to characterize extreme climate intensity, duration, and frequency (Donat et al.,

2016). The Expert Team on Climate Change Detection and Monitoring Indices (ETCCDMI) and the World Meteorological Organization (WMO) have developed several indicators for understanding climate extremes and trends (Zhang & Yang, 2004). The ETCCDMI-developed program RClindex was used to calculate the indices. Additionally, the climatic indices were chosen in light of their prior application in several Ethiopian locations by Mekasha et al. (2014), Geremew et al. (2020), and Wubaye et al. (2023). The existence of a significant trend was assessed at the significance levels of  $\alpha$  0.01 and  $\alpha$  0.05. A trend that is upward or downward is shown by positive or negative slope values, respectively. A thorough explanation of the extreme rainfall indices utilized in this investigation is found in Table 4.

As a spatial analysis technique, the selected extreme rainfall indices were constructed through inverse distance weighted (IDW) interpolation, which has shown high performance in mapping the spatial distribution of rainfall in space (Bayable et al., 2021). The weighted mean of a known site is assumed to be the value of an unknown place when using the IDW spatial interpolation technique. It assigns values based on distance weighting to unknown locations. Furthermore, the frequency of wet and arid years from 1981 to 2019 was examined using the standardized anomaly index (SAI). I used SAI to measure rainfall variation, which represents the deviation from the average rainfall over the studied years (Alemu & Bawoke, 2020). The following formula is used to compute the SAI:

**Table 4** Analysis of rainfall data from CHIRPS and meteorological stations at monthly and annual timescales

	Gondar	Dangila	Adet	Bahir Dar	Debre Tabor
Monthly timescale					
R	0.57	0.74	0.54	0.75	0.52
NSE	0.37	0.48	0.46	0.87	0.45
MAE	13.25	10.67	15.9	18.75	11.92
MBE	4.25	-6.83	13.08	13.76	1.07
RMSE	17.25	13.13	18.82	14.24	15.65
Annual time scale					
R	0.57	0.74	0.52	0.46	0.52
NSE	0.27	0.38	0.45	0.17	0.15
MAE	58.86	28.09	80.3	87.1	42.92
MBE	51.15	-61.9	56.95	-31.35	12.92
RMSE	86.98	57.56	25.5	32.99	87.7

$$SAI_i = \frac{Y_i - \bar{Y}}{\sigma} \tag{5}$$

In this equation, SAI<sub>i</sub> represents the standardized anomaly in year *i*, Y<sub>i</sub> represents the rainfall during that year,  $\bar{y}$  represents the long-term mean rainfall across the observation period, and  $\sigma$  represents the standard abnormality of rainfall throughout the observation period. In analysis, negative values indicate drought, and positive values indicate above-average

precipitation or a wet situation (Alemu & Bawoke, 2020). A classification system proposed by Funk et al. (2015) was employed to define dry or wet intensity. According to Funk et al. (2015), the SAI value is categorized as extremely wet (SAI > 2), extremely dry (SAI ≤ -2), very wet (1.5 ≤ SAI ≤ 1.99), very dry (-1.99 ≤ SAI ≤ -1.5), moderately moist (1 ≤ SAI ≤ 1.49), moderately dry (-1.49 ≤ SAI ≤ -1), and normal (-0.99 ≤ SAI ≤ 0.99).

### Results and discussion

#### Comparison of CHIRPS and the station’s rainfall data

The efficiency of CHIRPS rainfall records was evaluated on the monthly and yearly periods by comparing them with station observations. Table 5 illustrates statistical comparison results on both a monthly and annual scale. The disparity between monthly and annual mean rainfall values at the station and CHIRPS is presented in Figs. 2 and 3, respectively. The NSE for every station site was between 0.37 and 0.87 based on monthly rain gauge and CHIRPS rainfall data. Additionally, all station locations had correlation coefficient values (*r*) between 0.52 and 0.75. (Table 2). Bahir Dar station locations showed a correlation coefficient of 0.75 and NSE of 0.87, indicating

**Table 5** Trends of the analyzed extreme rainfall indices in LTSB

No	Stations	Rx1day	Rx5day	SDII	R10mm	R20mm	CDD	CWD	R95p	R99p	PRCPTOT
1	Achefer	-0.009	-0.368	-0.017	0.149	-0.141	0.092	-0.252*	-1.622	0.129	2.281
2	Addis Zemen	0.06	0.102	0	0.158	0.047	0.474	-0.294*	0.454	0.227	3.078
3	Bahir Dar	-0.182	-0.097	-0.033	0.196	-0.116*	0.418	0.033	-2.854*	-1.946a	2.972
4	Dangila	-0.052	-0.17	-0.007	0.155	-0.055	-0.195	-0.274*	-1.849	-0.588	1.546
5	Debre Tabor	-0.107	0.058	0	0.401a	0.179	0.36	-0.234	-0.852	-0.566	6.49a
6	Delgi	-0.092	-0.163	-0.016	-0.012	-0.003	0.964	-0.265*	-0.002	-0.785	1.936
7	Dembia	-0.252	-0.294	-0.018	0.152	0.027	0.358	-0.091	-0.044	-0.182	3.809a
8	Dengel Ber	-0.058	0.098	-0.009	-0.012	0.061	0.166	-0.141	-0.134	-0.205	4.029*
9	Dera	-0.065	-0.325	-0.027	0.238*	-0.025	0.053	0.043	-1.189	-0.418	4.385*
10	Gondar	0.006	-0.043	0.007	0.127	0.02	0.085	-0.246	1.371	-0.46	4.03*
11	Merawi	-0.104	-0.228	-0.002	0.071	-0.032	-0.698	-0.267a	0.46	-0.491	1.636
12	Meshenti	-0.383*	-0.045	-0.043	0.219*	-0.073	-0.986	-0.023	-2.698*	-2.457a	2.549
13	Sekela	-0.14	0.037	-0.006	0.16	0.041	-0.259	-0.256*	0.601	-0.015	3.382
14	Tana	-0.052	-0.154	-0.023	0.071	-0.004	-0.267	-0.139	-0.795	-0.429	3.045
15	Woreta	-0.111	-0.144	-0.02	0.236*	0.111	0.151	-0.082	-1.793	-0.457	4.798*

a and \* are significant trends at  $\alpha$  0.01 and  $\alpha$  0.05

a very high degree of compatibility with the station records. In contrast, there were relatively low correlation coefficients (0.52) and Nash–Sutcliffe efficiency (0.34) at the Debre Tabor and Gondar weather stations.

Furthermore, CHIRPS rainfall estimates performed well when compared with station rainfall data using MAE, MBE, and RMSE values (Table 5). As presented in the table, the maximum (minimum) MAE, MBE, and RMSE were 18.75 (10.67), 13.76 (1.07), and 17.25 (13.13) mm/month, respectively, on monthly timescales. There was a maximum MAE (18.75 mm/month) and a minimum MAE (10.67 mm/month) recorded at the Bahir Dar and Dangila station locations. Table 5 shows that the monthly CHIRPS rainfall products for the Dangila station were underestimated by approximately 6.83 mm/month. While the CHIRPS monthly rainfall data at Bahir Dar and Adet stations were overestimated by about 13.76 mm

and 13.08 mm, respectively. The highest RMSE (18.82 mm/month) was recorded at the Adet station location, while the lowest (13.13) was recorded at the Dangila station location. Overall, the assessments of the MBE, RMSE, and MAE were lower on mean monthly timescales than on annual timescales. Based on the overall performance assessment of monthly rainfall estimates, CHIRPS's rainfall data appear to be valuable for applications such as spatial and temporal examination of rainfall extremes trends. It was found that the results for the comparison by using monthly rainfall output from CHIRPS with climate stations were identical to those obtained from previous studies conducted via Bayable et al. (2021) in West Harerge, Alemu and Bawoke (2020) in the Ethiopian Amhara region, Ayehu et al. (2018) in Ethiopia's UBNB, and Dinku et al. (2018) in East Africa. Moreover, this study confirmed previous findings (e.g. Bayable et al., 2021; Dinku et al., 2018) conducted in most parts

**Fig. 2** A comparison of CHIRPS rainfall data with meteorological station rainfall data based on the LTSB mean monthly rainfall

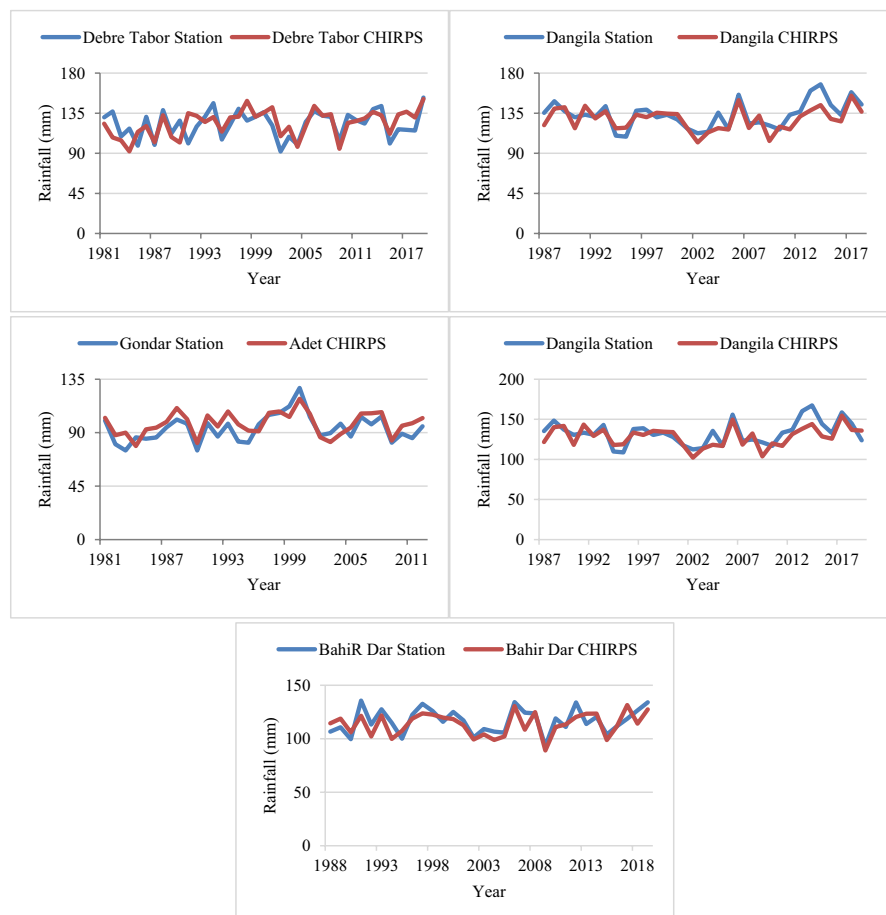
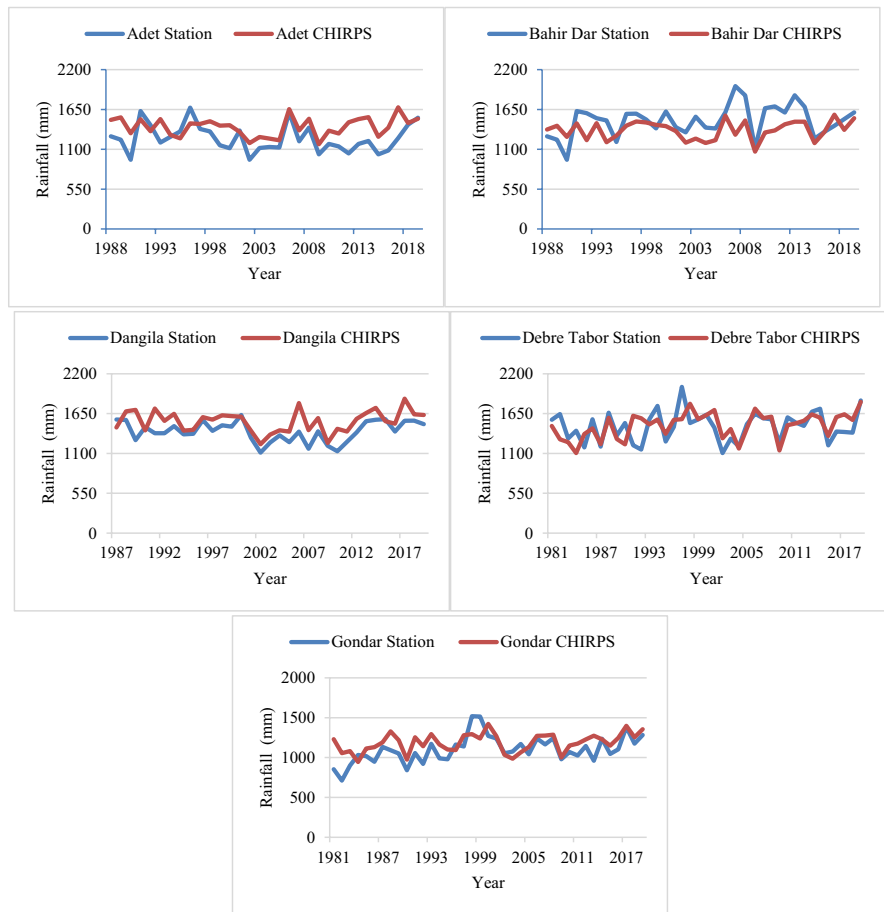




**Fig. 3** Comparison of CHIRPS rainfall estimate with rain gauge data based on the annual rainfall in LTSB



of Ethiopia using monthly rainfall data. A study by Ageet et al. (2022) for Equatorial East Africa also found that CHIRPS performed better than other models in estimating monthly rainfall. Superior CHIRPS performance has also been found in Columbia, Northwestern South America (Valencia et al., 2023). The monthly temporal scale rainfall amount estimated by CHIRPS forms increasingly precise and close to the reference data. Similarly, another study in Ethiopia (Gashaw et al., 2023) found that CHIRPS performed better at the monthly scale than at the annual timescale. Therefore, CHIRPS precipitation data can reproduce the LTSB rainfall pattern and be used for further climate analysis.

CHIRPS rainfall estimate was also assessed and displayed in Table 5 for the LTSB in annual timescales for each ground-based rainfall data and CHIRPS satellite estimate. Figure 3 illustrates the variation between the station’s recorded annual rainfall and that estimated by the CHIRPS satellite

estimate. Similar to the monthly timescale, CHIRPS estimates and weather station measurements showed excellent agreement, with correlation coefficients ( $r$ ) ranging between 0.46 and 0.74. CHIRPS also showed NSE values between 0.15 and 0.45 and RMSE values between 25.5 and 87.7. The maximum overestimation (minimum underestimation) was 56.95 (−61.9) mm/year in Adet (Dangila) station locations of the sub-basin. A maximum (minimum) MAE of 87.1 (28.09) mm/year was observed at Bahir Dar (Dangila) station locations. Mohammed and Yimam (2022) also report that CHIRPS performs better for estimating annual rainfall in the Beshilo subbasin of UBNB, and Gashaw et al. (2023) in South Ethiopia, Bayable et al. (20213) in West Harerge, and Alemu and Bawoke (2017) in Ethiopian Amhara. The superior performance of CHIRPS for generating annual rainfall across LTSB by entire/majority performance metrics in this study is consistent with the findings obtained in East Africa (Ageet et al., 2022). Furthermore,

Valencia et al. (2023) found that the CHIRPS estimate is superior to other satellite estimates in simulating annual rainfall over different altitude zones in Colombia (North Western South America).

#### Temporal trends of extreme rainfall in LTSB

The Extreme Rainfall Detection Monitoring and Indices (ETCCDMI) provides information regarding extreme rainfall indicators, associated with rainfall types, frequency, intensity, and extremes (Zhang & Yang, 2004). Table 6 shows time series trend analyses of ten extreme rainfall indices estimated over 1981–2019. In addition, the temporal trends of the selected rainfall intensity indices for the entire basin over the period 1981–2019 are shown in Figs. 4 and 5. The majority (86.66%) of the studied station locations had declining trends in Rx-1DAY rainfall while only Addis Zemen and Gondar stations had positive trends (Table 6). Even so, the trend that was significant (at  $\alpha=0.01$ ) was only at the Meshenti location of the station (Table 6). The minimum value for the Rx-1DAY trend magnitude was  $-0.009$  mm/month at the Achefer (southwestern part of the basin) station location (Fig. 7). Similar trend analysis to Rx-1DAY was made for the indexes of maximum Rx5day rainfall (which could indicate flood-producing events). A negative insignificant (at  $\alpha$  0.01 and 0.05) trend was observed at 73.33% of the sites studied, while an insignificant increase was seen at the remaining sites. The slope of the decreasing trends in Rx5day in the LTSB varied from  $-0.043$  to  $-0.294$  mm/month, with the highest record being found at the Dmbia stations of the basin (Table 6 and Fig. 7). On the contrary, there were increasing trends in Addis Zemen, Debre Tabor, Dengel Ber, and Sekela station

locations with magnitudes of 0.102, 0.058, 0.098, and 0.037, respectively.

Except for an insignificant trend at 6.66% and no trend at 13.33%, SDII trends declined at most studied station locations (Table 7). The results of trend magnitudes for stations with significant changes in R10mm and R20mm at significant levels of 0.05 or 0.01 are analyzed in (Table 6). Rainfall intensity is measured by the annual count of days with daily rainfall of 10 and 20 mm or above. This is also known as the R10mm and R20mm indices. The majority of stations' locations (86.66%) showed an increase in R10mm, while R20mm had divergent trends. R10mm rose significantly (at  $\alpha$  0.01) at Dera, Meshenti, and Woreta, and significantly (at  $\alpha$  0.05) at Debretabor, with magnitudes ranging from 0.219 to 0.401 days/year. There is a likely risk of flooding and soil erosion around the station area if these indices increase. In contrast, the R20mm indices trend analysis revealed that there was a substantial decline in the Bahir Dar station location with a magnitude of  $-0.116$ .

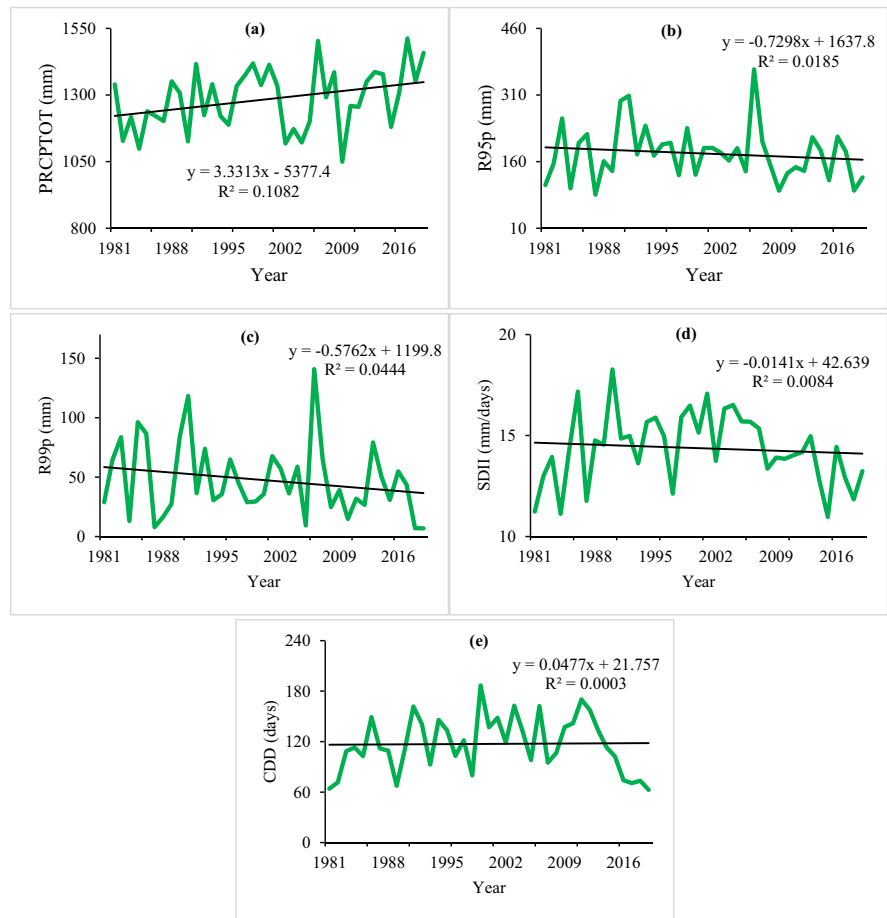
Using CDD and CWD, the researcher measured the presence and absence of rainfall greater than 1 mm. For CDD, 66.66% of climate station locations showed an insignificant positive trend, while 33.33% exhibited a declining trend (Table 7). The intensity of the insignificant positive trend of CDD varies between 0.053 and 0.964 days/year, with the highest magnitude found at the Delgi station location. While negative trends were observed at five locations of the station, fluctuating between  $-0.195$  and  $-0.986$  days/year with the highest magnitude observed at the Meshenti station location (Table 6 and Fig. 7). CWD trends are typically negative throughout the basin, with 40% of stations indicating significantly declining trends (at  $\alpha$  0.01) for Achefer, Addis Zemen, Dangila, Delgi, and Merawi (at  $\alpha$  0.05) with magnitudes

**Table 6** Summary of trend results for extreme indices

Trend type	RX1day	Rx5day	SDII	R10mm	R20mm	CDD	CWD	R95p	R99p	PRCPTOT
%↑	13.33	26.66	6.66	86.66	46.66	66.66	13.33	26.66	13.33	100
%↓	86.66	73.33	80	13.33	53.33	33.33	86.66	73.33	86.66	0
%↑*	0	0	0	26.66	0	0	0	0	0	40
%↓*	6.66	0	0	0	6.66	0	40	13.33	13.33	0
%nt	0	0	13.33	0	0	0	0	0	0	0

%↑, percent of stations with an increasing trend; %↓, percent of stations with a decreasing trend; %↑\*, percent of stations with a significant increasing trend at  $\alpha$  0.01 and  $\alpha$  0.05; and %↓\*, percent of stations with the significant decreasing trend at  $\alpha$  0.01 and  $\alpha$  0.05

**Fig. 4** Average sub-basin-wide trends in excessive rainfall indices. **a** PRCP-TOT, **b** R95p, **c** R99p, **d** SDII, and **e** CDD from



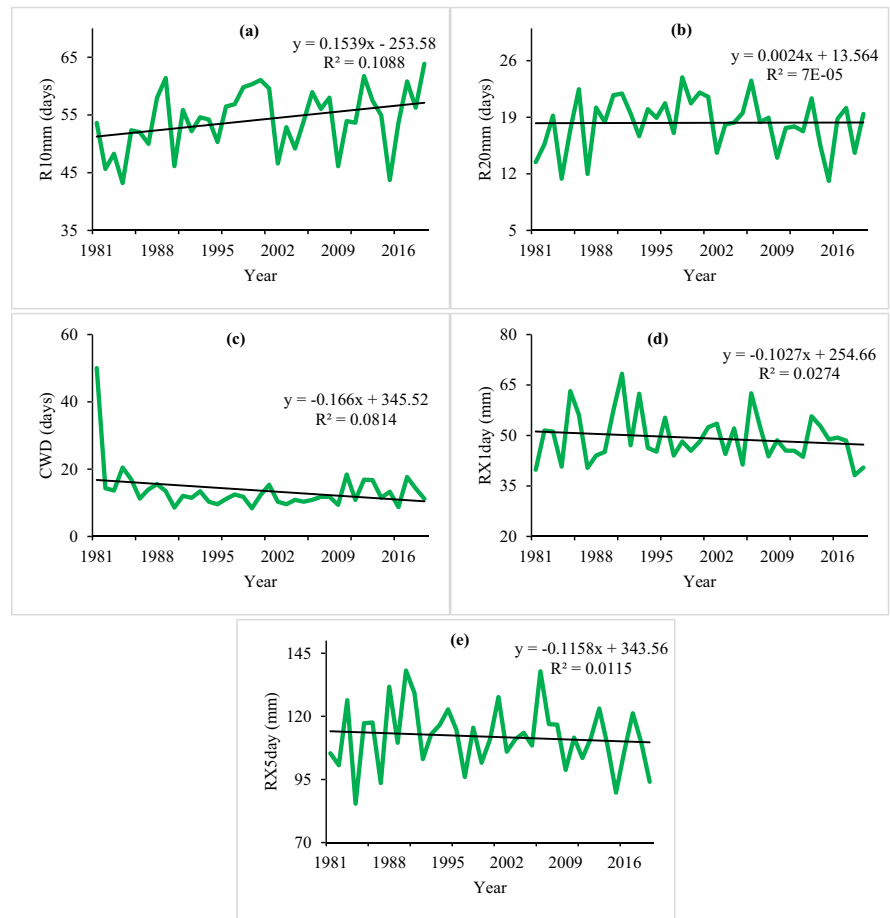
ranging from 0.252 to 0.294 days/year. The results suggest that aridity is increasing at these stations.

The daily rainfall series at a station’s location was also employed to compute percentile-based indices such as R99p and R95p, where the total rainfall exceeds a certain percentile value. The results of trend analyses indicate that both R99p and R95p are decreasing over the LTSB (Fig. 4). Based on the RCLimindex test results, R99p and R95p indicated a rising trend at 86.66% and 73.33 stations, respectively. Significant ( $\alpha=0.01$ ) downward trends in R99p were detected in Bahir Dar (1.946 days/year) and Meshenti (2.457 days/year). Bahir Dar and Meshenti stations also showed negative significant (at  $\alpha$  0.01) trends for R95p with magnitudes of 2854 and 2698 mm/year, respectively. A trend analysis of PRCP-TOT (Fig. 6) shown an upward result through all stations. Consequently, the total rainfall at Debre Tabor, Dembia, Dengel Ber, Dera, Gondar, and Woreta significantly

(at  $\alpha$  0.01 and 0.05) increased by 6.49, 3.8, 4.029, 4.385, 4.03, and 4.71 mm/year, respectively. In the entire sub-basin, extreme rainfall indices decreased except for R10mm, CDD, and PRCP-TOT (Table 7). Due to these divergent extreme rainfall trends, the LTSB’s trend cannot be considered stable. Extreme rainfall events may damage socio-economic activities and ecosystems.

The results of the analysis of excessive rainfall events through the LTSB indicate that most are decreasing, with the exception of PRCP-TOT, R10mm, and CDD (Tables 6 and 7). Previous studies on rainfall indices in Ethiopia have drawn similar conclusions. Berhane et al. (2020) concluded that extreme rainfall events decreased in the semi-arid parts of Western Tigray for most of the analyzed extreme rainfall indices. Their findings revealed a significant (at  $\alpha$  0.01 and 0.05) decline in R95p, R20, R95p, Rx5day, and R99p throughout their study region. The result from this

**Fig. 5** Average sub-basin-wide trends in the selected rainfall indices. **a** R10 mm, **b** R20 mm, **c** CWD, **d** RX1day, and **e** RX5day



study is in contradistinction from those of other studies investigating a growing trend of excessive rainfall events (Wubaye et al., 2023; Worku et al., 2019). For instance, Wubaye et al. (2023) detected a rise in excessive rainfall events over Ethiopia from 1986 to 2020. This may be due to the fact that the existence of a variety of factors, including the study period, length of observation, and statistical methods.

The declining trends in CWD are also consistent with the findings of Berhane et al. (2020) and Gebrechorkos et al. (2019). Moreover, other researchers such as Teshome and Zhang (2019), Worku et al. (2019), Berhane et al. (2020), and Wubaye et al. (2023) have investigated a growing trend in PRCPTOT similar to our result. Generally, LTSB excessive rainfall events exist consistent with global trends in expressions of frequency, intensity, and spatial extent (IPCC, 2012, 2013). The trend in the occurrence, amount, and areal extent of rainfall extremes was found in the LTSB,

which is in concurrence with the global trend. It can be due to global anthropogenic climate change and other large- and local-scale factors. This is similar to previous studies by Wubaye et al. (2023), who reported continuous variability and increases in heavy rainy days across Ethiopia. It is also reported that the R10mm has increased 70% of the world's land area and added to the annual total rainfall amount (Alexander et al., 2006). A change in extreme rainfall incidences, like droughts, landslides, and floods can impact agriculture in multiple ways. Severe rainfall can have a destructive influence on smallholder farmers' crop production system, especially heavy storms, landslides, and flood events. An occurrence in the high flood disaster in the Fogera floodplain in 2006 resulted in a high rise in Lake Tana's water level (Moges & Moges, 2019). Conversely, extreme rainfall events reduce rainfall and water availability for crop production (Funk et al., 2012).

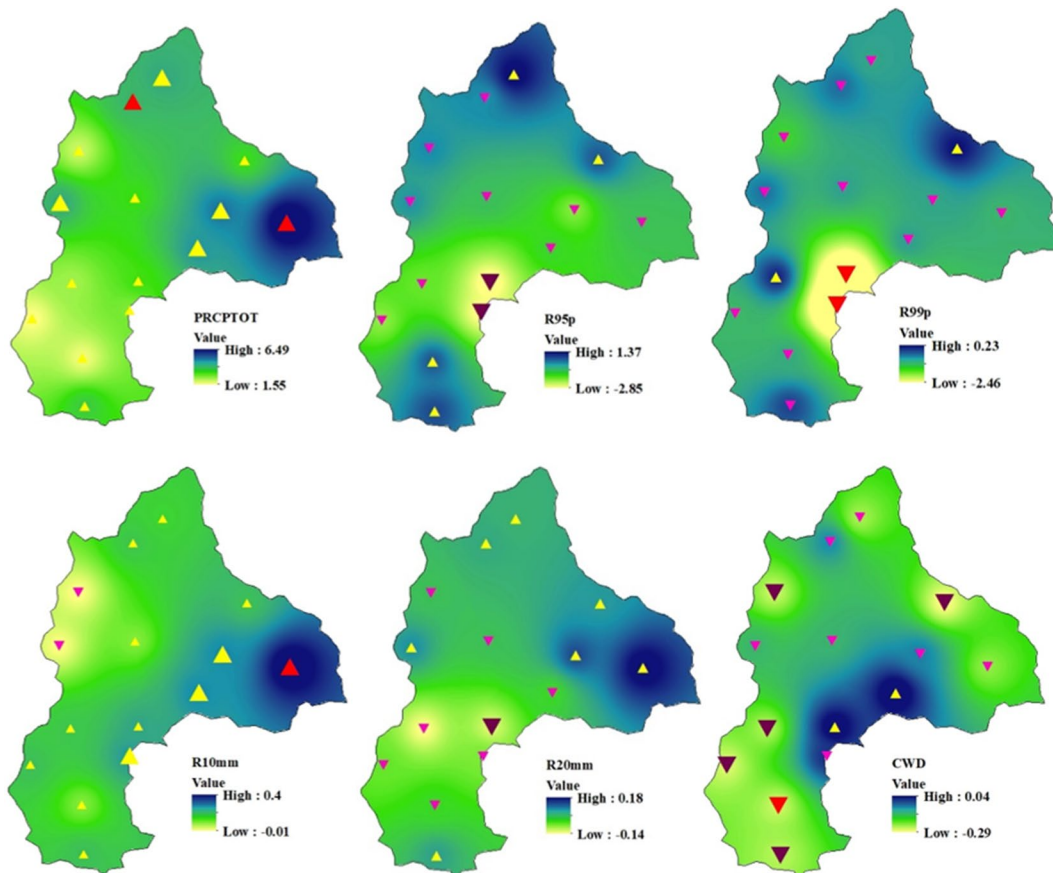


**Fig. 6** Spatial distribution of long-term trends in extreme indices (PRCPTOT, R95p, R99p, R10mm, R20mm, and CWD) of LTSB. The upright yellow and inverted pink triangles indicate increasing and decreasing trends, respectively. Triangles that

are red inverted or upright indicate significant trends that are increasing or decreasing at  $\alpha = 0.01$ . Large upright yellow triangles indicate significant increasing trends at  $\alpha = 0.05$ , while inverted purple triangles indicate significant decreasing trends

### Spatial trend results of excessive rainfall in LTSB

The researcher also examined the spatial distribution of excessive rainfall indices in addition to temporal analysis. Figure 6 shows the spatial dispersal of rainfall indices for (PRCPTOT, R95p, R99p, R10mm, R20mm, and CWD) for individual rainfall locations (gridded) during the period 1981–2019. The results of PRCPTOT revealed that the maximum rise was found at the Debre Tabor station situated in the Western portion of the LTSB; however, related to areas nearby Gondar (Northern), Dembia (Northern Central), and Delgi (Northwestern), where relatively moderate increases were observed (Fig. 6), there was a comparatively small increase around Dangila (South-western), Merawi (Southern Central), and

Delgi (North-western). The highest spatial unevenness of R95p was observed at Sekela (Southern), Merawi (Southern central), Gondar (Northern), Addis Zemen (North-eastern), and Meshenti (South-eastern). Likewise, the highest R99p reductions were perceived in the Bahir Dar and Meshenti (South-eastern) parts of the sub-basin.

The southeastern sections of the LTSB showed a relatively significant (at  $\alpha = 0.01$  and  $0.05$ ) increase in CWD, according to spatial analysis. In contrast, there was a reduction in other parts of LTSB. The largest R10mm increase was found in the eastern part of the LTSB. In contrast, the north-western portions of the sub-basin showed smaller R10mm reductions. A relatively high increasing trend in R20mm was also observed around Debre Tabor in the eastern portion

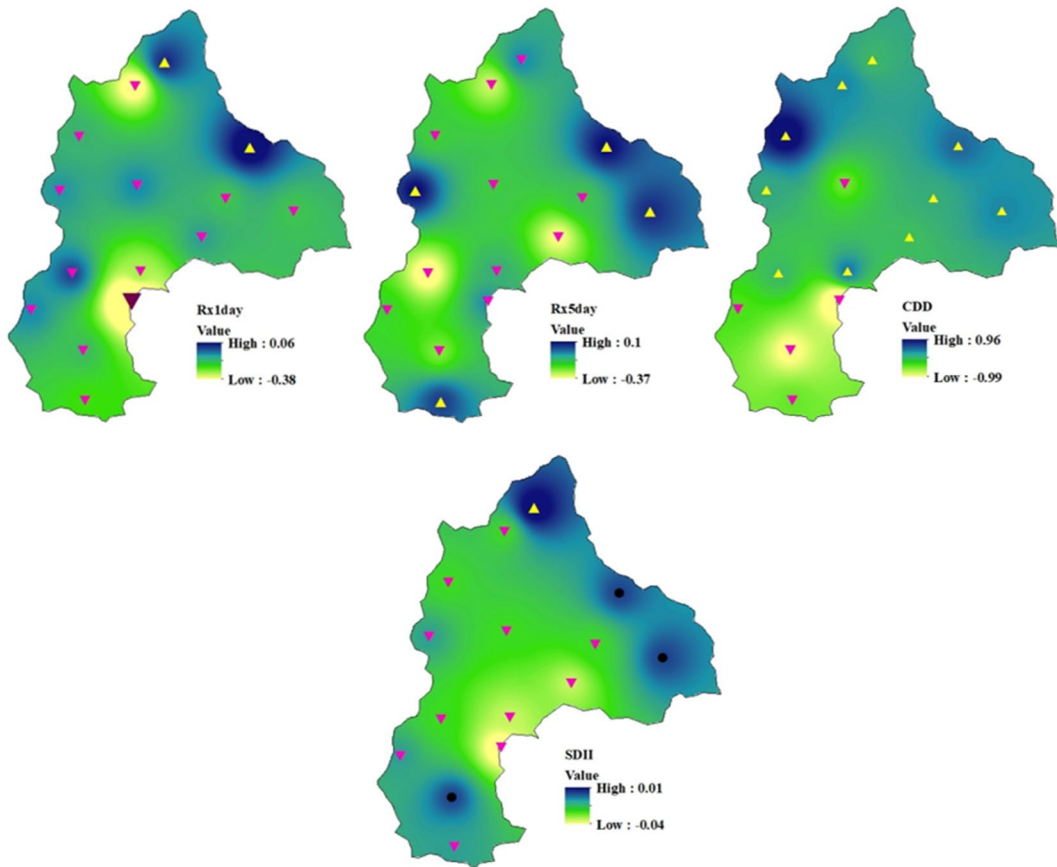


**Fig. 7** Spatial variations of long-term trends in excessive rainfall (RX1day, RX5day, CDD, and SDII) of LTSB. Triangles are the same as in Fig. 6. Indices with no trends are marked by black dots

of the LTSB. In contrast, there was a comparatively maximum decreasing trend around Achefer in the southwestern part of the sub-basin. Additionally, the results revealed the central areas of the LTSB experienced moderate changes on R20 mm, while the eastern and southern areas experienced the maximum and minimum changes.

Spatially, RX1day, RX5day, CDD, and SDII for individual rainfall locations over the period 1981–2019 are presented in Fig. 7. As elucidated in Fig. 7, the slope of rainfall indices, RX1day, covers a range of  $-0.38$  to  $0.06$  mm and is lowest in the southeastern section of the LTSB and highest in the northeast. The trend of RX5day was positive in the western, eastern, and northeastern areas of LTSB but decreased in the southwestern, north-center, and southeastern portions of the sub-basin. Figure 7 shows that CDD's spatial distribution ranges

from  $-0.97$  to  $0.96$  days. A minimum number of days occurred in the south-central and south-eastern parts, while a maximum number was observed in the northwestern region. South-east and south-central parts of the SDII within the sub-basin showed a similar decreasing trend as CDD, but the northern, east, and north-eastern parts exhibited no trend in the time series. This phenomenon indicates a decline in rainfall each day.

Figures 8 and 9 display the standardized mean anomaly values for each index throughout the whole sub-basin. The data presented indicates that the average deviation of rainfall indices across the sub-basin had a downward trend for all but PRCPTOT, CDD, and R10mm. All extreme rainfall indices, however, showed noticeable variations in their 5-year moving average and trend. The fact that the extreme rainfall trend is deviating suggests that there was instability

in the LTSB rainfall trend. This shows that in the sub-basin, excessive rainfall may harm ecosystems and socioeconomic activities.

Spatially, extreme rainfall indices indicate an irregular distribution of severe rainfall over the studied sub-basin. This study’s results agree with those of Teshome and Zhang (2019), Wubaye et al. (2023), and Worku et al. (2019) who conveyed continuous spatial unevenness in excessive rainfall indices throughout different areas in Ethiopia. Furthermore, Mekasha et al. (2014) reported that excessive rainfall indices at three Ethiopian eco-environments exhibited inconsistencies and were not significant. Similarly, the low spatial coherence of the found trends in rainfall extremes is similar to that observed in various areas across other continents (Agilan & Umamahesh, 2018; Bezerra et al., 2019; Cardell et al., 2020; Casanueva et al., 2014; Mladjic et al., 2011). Therefore, the observed spatial unevenness of excessive rainfall

indices could be portrayed by means of the country’s varied topography and relief features (Gebrechorkos et al., 2019; Mekasha et al., 2014; Mengistu et al., 2013). In addition, pressure systems in the Indian Ocean, equatorial Pacific, Gulf of Guinea, Mediterranean region, and Arabian Peninsula are responsible, as is the Intertropical Convergence Zone (ITCZ) and global climate change (Berhane et al., 2020; Worku et al., 2019).

Summary and conclusions

It has been shown in several studies that Ethiopia is vulnerable to climate change, which will likely increase disaster frequency and severity. There is potential for climate change to worsen economic and social conditions across the country. This is especially true for areas that depend heavily on rain-fed agriculture and have resources sensitive to climate

**Fig. 8** A time series depiction of the averaged extreme rainfall indices for the sub-basin. **a** PRCPTOT; **b** R95p; **c** R99p; **d** R10mm; and **e** is for R20mm. The black, curved line represents the 5-year moving average, while the red, straight line represents the variables’ linear trend

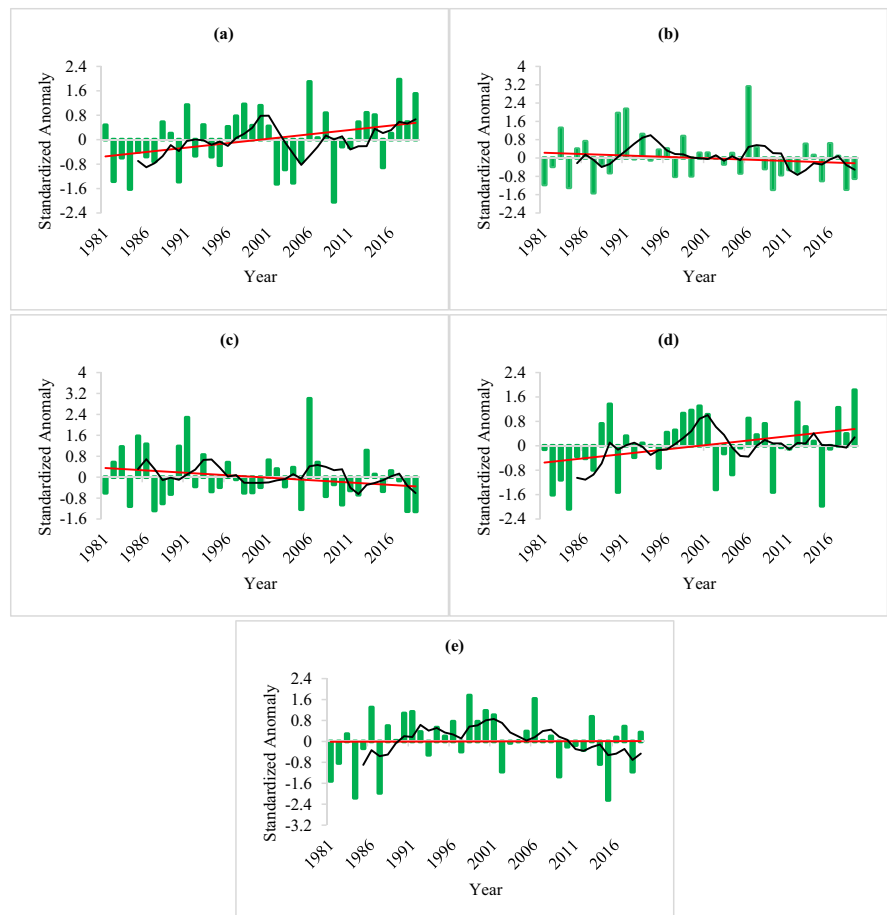
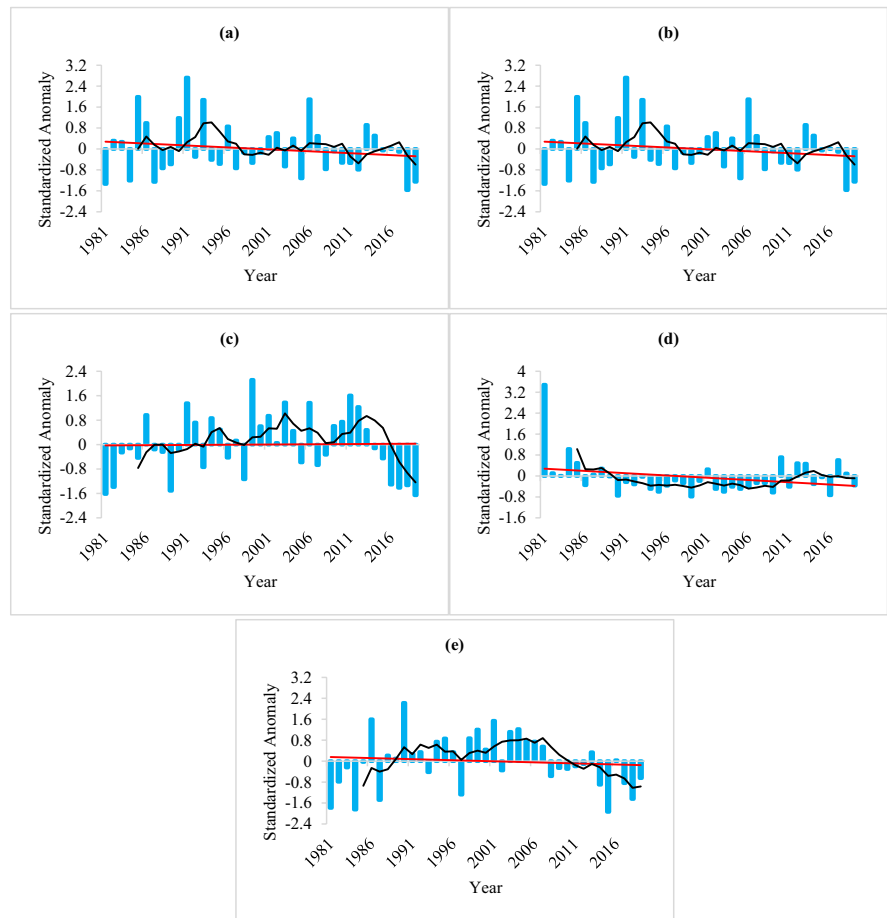


**Fig. 9** Time series plot of averaged sub-basin wide rainfall extreme indices. **a** RX1day, **b** RX5day, **c** CDD, **d** CWD, and **e** is for SDII. As in Fig. 8, the lines are identical



change. The extent, nature, and location of climate change and weather extremes can be reduced if information is available. This study examined the change in severe rainfall indices in the LTSB of the UBNB by CHIRPS rainfall estimate. To examine the historical variations in the extreme rainfall happenings in the last 39 years (1981–2019), the study uses WMO and ETCCDI extreme rainfall indices. For extracting the vector data of CHIRPS satellite rainfall outputs, I also employed Python 3.8.5 (Rossum & Drake, 2001). Before being used, CHIRPS gridded rainfall datasets were evaluated and validated against in situ observations to ensure data quality, uncertainty, and precision.

Almost all rainfall extreme indices indicate a decline in risky rainfall incidences, which can negatively impact the economy of stakeholders in the sub-basin. RX1day, CWD, and R99p, for example, revealed declining trends in 86.66% of climate

station locations. About 73.33% of the overall stations in RX5day and R95p also disclosed a declining trend. Meanwhile, only PRCPTOT, R10mm, and CDD unveiled a rising trend at 100%, 86.66%, and 66.66% of climate stations. A higher probability of seasonal droughts and increased dryness is indicated by the increasing trend of CDD. It increases transpiration from the plant and evaporation from water bodies. This dries up the soils and vegetation and decreases surface water. Increased flooding, crop damage, landslides, and soil erosion are possible outcomes of the observed rising trends of PRCPTOT and R10mm in the LTSB. This result disagrees with other studies that investigated an ascendant trend in extreme rainfall indices. The difference in the trend of extreme indices among studies could be attributed to the change in the study period and study area, length of observation, and statistical methods used to measure trends.



Furthermore, extreme rainfall trends show substantial spatiotemporal variability between stations. The results found in this study are reliable with former studies that have concluded a spatially inhomogeneous pattern of rainfall indices in different regions of Ethiopia. Along with the reduction tendency in extreme indices of rainfall, the average standardized anomaly index over the sub-basin showed that negative anomalies exceeded positive anomalies throughout the study age. In conclusion, this study provided profound evidence of the high spatial and historical variation of rainfall intensity and frequency in the LTSB. Rain-dependent smallholders must therefore prepare for climate change and modify their agricultural practices to account for extreme rainfall variability. However, because of a lack of time and funding, it was difficult to determine the particular adaptation and mitigation strategies for extreme rainfall in this study. As a result, additional research is required to investigate practical insights and policy implications based on the findings of this study.

**Acknowledgements** The research is self-motivated and not funded. This study owes a great deal of thanks to the Ethiopian National Meteorological Agency (NMA) for providing station data for validation. The authors are also appreciative to the journal's editor and the anonymous reviewers for their constructive suggestions, which helped to improve the paper's quality.

**Data availability** The authors are not permitted to share the observed rainfall data because it was obtained from the NMA; it is solely for personal use. However, the employed CHIRPS rainfall data can be accessed on their website and given up on resealable requests.

**Competing interests** The authors declare no competing interests.

**Declarations** Ethical responsibilities of authors.

The author have read, understood, and have complied as applicable with the statement on "Ethical responsibilities of Authors" as found in the Instructions for Authors.

## References

- Ademe, D., Zaitchik, B. F., Tesfaye, K., Simane, B., Alemayehu, G., & Adgo, E. (2020). Climate trends and variability at adaptation scale: Patterns and perceptions in an agricultural region of the Ethiopian Highlands. *Weather and Climate Extremes*, 29, 100263. <https://doi.org/10.1016/j.wace.2020.100263>
- Ageet, S., Fink, A. H., Maranan, M., Diem, J. E., Hartter, J., Ssali, A. L., & Ayabagabo, P. (2022). Validation of satellite rainfall estimates over equatorial East Africa. *Journal of Hydrometeorology*, 23(2), 129–151. <https://doi.org/10.1175/JHM-D-21-0145.1>
- Agilan, V., & Umamahesh, N. V. (2018). El Niño Southern Oscillation cycle indicator for modeling extreme rainfall intensity over India. *Ecological Indicators*, 84, 450–458. <https://doi.org/10.1016/j.ecolind.2017.09.012>
- Alemu, M. M., & Bawoke, G. T. (2020). Analysis of spatial variability and temporal trends of rainfall in Amhara region, Ethiopia. *Journal of Water and Climate Change*, 11(4), 1505–1520. <https://doi.org/10.2166/wcc.2019.084>
- Alexander, L. V., Zhang, X., Peterson, T. C., Caesar, J., Gleason, B., Klein Tank, A. M. G., & Vazquez-Aguirre, J. L. (2006). Global observed changes in daily climate extremes of temperature and precipitation. *Journal of Geophysical Research: Atmospheres*, 111(D5). <https://doi.org/10.1029/2005JD006290>
- Almazroui, M., Ashfaq, M., Islam, M. N., Rashid, I. U., Kamil, S., Abid, M. A., ... & Sylla, M. B. (2021). Assessment of CMIP6 performance and projected temperature and precipitation changes over South America. *Earth Systems and Environment*, 5(2), 155–183. <https://doi.org/10.1007/s41748-021-00233-6>
- Almazroui, M., Saeed, F., Saeed, S., Nazrul Islam, M., Ismail, M., Klutse, N. A. B., & Siddiqui, M. H. (2020). Projected change in temperature and precipitation over Africa from CMIP6. *Earth Systems and Environment*, 4, 455–475. <https://doi.org/10.1007/s41748-020-00161-x>
- Asfaw, A., Simane, B., Hassen, A., & Bantider, A. (2018). Variability and time series trend analysis of rainfall and temperature in northcentral Ethiopia: A case study in Woleka sub-basin. *Weather and Climate Extremes*, 19, 29–41. <https://doi.org/10.1016/j.wace.2017.12.002>
- Avtar, R., Komolafe, A. A., Kouser, A., Singh, D., Yunus, A. P., Dou, J., ... & Kurniawan, T. A. (2020). Assessing sustainable development prospects through remote sensing: A review. *Remote sensing applications: Society and environment*, 20, 100402. <https://doi.org/10.1016/j.rsase.2020.100402>
- Ayehu, G. T., Tadesse, T., Gessesse, B., & Dinku, T. (2018). Validation of new satellite rainfall products over the upper Blue Nile basin. *Ethiopia. Atmospheric Measurement Techniques*, 11(4), 1921–1936. <https://doi.org/10.5194/amt-11-1921-2018>
- Bayable, G., Amare, G., Alemu, G., & Gashaw, T. (2021). Spatiotemporal variability and trends of rainfall and its association with Pacific Ocean Sea surface temperature in West Harerge Zone. *Eastern Ethiopia. Environmental Systems Research*, 10(1), 1–21. <https://doi.org/10.1186/s40068-020-00216-y>
- Bayissa, Y. A., Moges, S. A., Xuan, Y., Van Andel, S. J., Maskey, S., Solomatine, D. P., ... & Tadesse, T. (2015). Spatio-temporal assessment of meteorological drought under the influence of varying record length: The case of upper Blue Nile basin, Ethiopia. *Hydrological Sciences Journal*, 60(11), 1927–1942. <https://doi.org/10.1080/02626667.2015.1032291>
- Bayissa, Y., Tadesse, T., Demisse, G., & Shiferaw, A. (2017). Evaluation of satellite-based rainfall estimates and application to monitor meteorological drought for the upper Blue Nile basin. *Ethiopia. Remote Sensing*, 9(7), 669. <https://doi.org/10.3390/rs9070669>

- Belay, A. S., Fenta, A. A., Yenehun, A., Nigate, F., Tilahun, S. A., Moges, M. M., ... & Walraevens, K. (2019). Evaluation and application of multi-source satellite rainfall product CHIRPS to assess spatio-temporal rainfall variability on data-sparse western margins of Ethiopian highlands. *Remote Sensing*, 11(22), 2688. <https://doi.org/10.3390/rs11222688>
- Berhane, A., Hadgu, G., Worku, W., & Abrha, B. (2020). Trends in extreme temperature and rainfall indices in the semi-arid areas of Western Tigray. *Ethiopia. Environmental Systems Research*, 9(1), 1–20. <https://doi.org/10.1186/s40068-020-00165-6>
- Bezerra, B. G., Silva, L. L., Santos e Silva, C. M., & de Carvalho, G. G. (2019). Changes of precipitation extremes indices in São Francisco River Basin, Brazil from 1947 to 2012. *Theoretical and Applied Climatology*, 135, 565–576. <https://doi.org/10.1007/s00704-018-2396-6>
- Bhaga, T. D., Dube, T., Shekede, M. D., & Shoko, C. (2020). Impacts of climate variability and drought on surface water resources in Sub-Saharan Africa using remote sensing: A review. *Remote Sensing*, 12(24), 4184. <https://doi.org/10.3390/rs12244184>
- Buuren, K.G.-O. (2015). Mice: Multivariate imputation by chained equations in R. *Journal of Statistical Software*, 45(3), 1–67.
- Cardell, M. F., Amengual, A., Romero, R., & Ramis, C. (2020). Future extremes of temperature and precipitation in Europe derived from a combination of dynamical and statistical approaches. *International Journal of Climatology*, 40(11), 4800–4827. <https://doi.org/10.1002/joc.6490>
- Casanueva, A., Rodríguez-Puebla, C., Frías, M. D., & González-Reviriego, N. (2014). Variability of extreme precipitation over Europe and its relationships with teleconnection patterns. *Hydrology and Earth System Sciences*, 18(2), 709–725. <https://doi.org/10.5194/hess-18-709-2014>
- Chakilu, G. G., Sándor, S., Zoltán, T., & Phinzi, K. (2022). Climate change and the response of streamflow of watersheds under the high emission scenario in Lake Tana sub-basin, upper Blue Nile basin. *Ethiopia. Journal of Hydrology: Regional Studies*, 42, 101175. <https://doi.org/10.1016/j.ejrh.2022.101175>
- Cohen, J. L., Furtado, J. C., Barlow, M., Alexeev, V. A., & Cherry, J. E. (2012). Asymmetric seasonal temperature trends. *Geophysical Research Letters*, 39(4). <https://doi.org/10.1029/2011GL050582>
- Dembélé, M., & Zwart, S. J. (2016). Evaluation and comparison of satellite-based rainfall products in Burkina Faso, West Africa. *International Journal of Remote Sensing*, 37(17), 3995–4014. <https://doi.org/10.1080/01431161.2016.1207258>
- Dendir, Z., & Birhanu, B. S. (2022). Analysis of observed trends in daily temperature and precipitation extremes in different agroecologies of gurage zone, southern Ethiopia. *Advances in Meteorology*, 2022. <https://doi.org/10.1155/2022/4745123>
- Dinku, T., Funk, C., Peterson, P., Maiment, R., Tadesse, T., Gadain, H., & Ceccato, P. (2018). Validation of the CHIRPS satellite rainfall estimates over eastern Africa. *Quarterly Journal of the Royal Meteorological Society*, 144, 292–312. <https://doi.org/10.1002/qj.3244>
- Dinku, T., Hailemariam, K., Maiment, R., Tarnavsky, E., & Connor, S. (2014). Combined use of satellite estimates and rain gauge observations to generate high-quality historical rainfall time series over Ethiopia. *International Journal of Climatology*, 34(7), 2489–2504. <https://doi.org/10.1002/joc.3855>
- Donat, M. G., Lowry, A. L., Alexander, L. V., O’Gorman, P. A., & Maher, N. (2016). More extreme precipitation in the world’s dry and wet regions. *Nature Climate Change*, 6(5), 508–513. <https://doi.org/10.1038/nclimate2941>
- Fenta, A. A., Yasuda, H., Shimizu, K., Ibaraki, Y., Haregeweyn, N., Kawai, T., ... & Ebabu, K. (2018). Evaluation of satellite rainfall estimates over the Lake Tana basin at the source region of the Blue Nile River. *Atmospheric Research*, 212, 43–53. <https://doi.org/10.1016/j.atmosres.2018.05.009>
- Funk, C., Peterson, P., Landsfeld, M., Pedreros, D., Verdin, J., Shukla, S., ... & Michaelsen, J. (2015). The climate hazards infrared precipitation with stations—A new environmental record for monitoring extremes. *Scientific data*, 2(1), 1–21. <https://doi.org/10.1038/sdata.2015.66>
- Funk, C., Rowland, J., Eilerts, G., Kebebe, E., Biru, N., White, L., & Galu, G. (2012). A climate trend analysis of Ethiopia. *US Geological Survey, Fact Sheet*, 3053(5), 6.
- Gashaw, T., Worqlul, A. W., Lakew, H., Taye, M. T., Seid, A., & Hailelassie, A. (2023). Evaluations of satellite/reanalysis rainfall and temperature products in the Bale Eco-Region (Southern Ethiopia) to enhance the quality of input data for hydro-climate studies. *Remote Sensing Applications: Society and Environment*, 31, 100994. <https://doi.org/10.1016/j.rsase.2023.100994>
- Gebrechorkos, S. H., Hülsmann, S., & Bernhofer, C. (2019). Changes in temperature and precipitation extremes in Ethiopia, Kenya, and Tanzania. *International Journal of Climatology*, 39(1), 18–30. <https://doi.org/10.1002/joc.5777>
- Geremew, G. M., Mini, S., & Abegaz, A. (2020). Spatiotemporal variability and trends in rainfall extremes in Enebsie Sar Midir district, northwest Ethiopia. *Modeling Earth Systems and Environment*, 6, 1177–1187. <https://doi.org/10.1007/s40808-020-00749-2>
- Gummadi, S., Rao, K. P. C., Seid, J., Legesse, G., Kadiyala, M. D. M., Takele, R., ... & Whitbread, A. (2018). Spatio-temporal variability and trends of precipitation and extreme rainfall events in Ethiopia in 1980–2010. *Theoretical and Applied Climatology*, 134, 1315–1328. <https://doi.org/10.1007/s00704-017-2340-1>
- Hagos, S. M., Leung, L. R., Yoon, J. H., Lu, J., & Gao, Y. (2016). A projection of changes in landfalling atmospheric river frequency and extreme precipitation over western North America from the Large Ensemble CESM simulations. *Geophysical Research Letters*, 43(3), 1357–1363. <https://doi.org/10.1002/2015GL067392>
- IPCC. (2012). Managing the Risks of Extreme Events and Disasters to Advance Climate Change Adaptation. In C. B. Field, V. Barros, T. F. Stocker, D. Qin, D. J. Dokken, K. L. Ebi, M. D. Mastrandrea, K. J. Mach, G.-K. Plattner, S.

- K. Allen, M. Tignor, & P. M. Midgley (Eds.), *A Special Report of Working Groups I and II of the Intergovernmental Panel on Climate Change* (p. 582). Cambridge, UK, and New York, NY, USA: Cambridge University Press.
- IPCC. (2013). *Climate Change 2013: the Physical Science Basis*. In T. F. Stocker, D. Qin, G.-K. Plattner, M. Tignor, S. K. Allen, J. Boschung, A. Nauels, Y. Xia, V. Bex, & P. M. Midgley (Eds.), *Contribution of Working Group I to the Fifth Assessment Report of the Intergovernmental Panel on Climate Change* (p. 1535). Cambridge, United Kingdom and New York, NY, USA: Cambridge University Press.
- IPCC. (2018). *Climate Change 2018: Impact of 1.5°C Global Warnings on Natural and Human Systems*. In P. Zhai, H.-O. Portner, D. Roberts, J., Skea, P. R. Shukla, A. Pirani, W. Moufouma-Okia, C. Peans, R. Pidcock, S. Connors, J. B. R. Matthews, Y. Chen, X. Zhou, M. I. Gomis, E. Lonnoy, T. Maycock, M. Tignor, T. Waterfield (Eds.), *Masson-Delmotte V.* (in press).
- IPCC. (2021). *Summary for policymakers*. In V. Masson-Delmotte, P. Zhai, A. Pirani, S. L. Connors, C. Péan, S. Berger, N. Caud, Y. Chen, L. Goldfarb, M. I. Gomis, M. Huang, K. Leitzell, E. Lonnoy, J. B. R. Matthews, T. K. Maycock, T. Waterfield, O. Yelekçi, R. Yu, B. Zhou (Eds.), *Climate Change 2021: the Physical Science Basis. Contribution of Working Group I to the Sixth Assessment Report of the Intergovernmental Panel on Climate Change*. Cambridge University Press. (in press).
- Jothimani, M., Abebe, A., & Dawit, Z. (2020). Mapping of soil erosion-prone sub-watersheds through drainage morphometric analysis and weighted sum approach: A case study of the Kulfo River basin, Rift valley, Arba Minch, Southern Ethiopia. *Modeling Earth Systems and Environment*, 6, 2377–2389. <https://doi.org/10.1007/s40808-020-00820-y>
- Kimani, M. W., Hoedjes, J. C., & Su, Z. (2017). An assessment of satellite-derived rainfall products relative to ground observations over East Africa. *Remote Sensing*, 9(5), 430. <https://doi.org/10.3390/rs9050430>
- Mekasha, A., Tesfaye, K., & Duncan, A. J. (2014). Trends in daily observed temperature and precipitation extremes over three Ethiopian eco-environments. *International Journal of Climatology*, 34(6), 1990–1999. <https://doi.org/10.1002/joc.3816>
- Mengistu, K., Alemu, K., & Destaw, B. (2013). Prevalence of malnutrition and associated factors among children aged 6–59 months at Hidabu Abote District, North Shewa, Oromia Regional State. *J Nutr Disorders Ther*, 1(1), 2161–2509. <https://doi.org/10.4172/2161-0509.1000T1-001>
- Mladjic, B., Sushama, L., Khaliq, M. N., Laprise, R., Caya, D., & Roy, R. (2011). Canadian RCM projected changes to extreme precipitation characteristics over Canada. *Journal of Climate*, 24(10), 2565–2584. <https://doi.org/10.1175/2010JCLI3937.1>
- Moges, M. A., & Moges, S. A. (2019). Characteristics of future extreme precipitation and temperature in Lake Tana basin, Ethiopia. In *Extreme hydrology and climate variability* (pp. 59–69). Elsevier. <https://doi.org/10.1016/B978-0-12-815998-9.00006-3>
- Mohammed, J. A., Gashaw, T., Tefera, G. W., Dile, Y. T., Worqlul, A. W., & Addisu, S. (2022). Changes in observed rainfall and temperature extremes in the upper Blue Nile basin of Ethiopia. *Weather and Climate Extremes*, 37, 100468. <https://doi.org/10.1016/j.wace.2022.100468>
- Mohammed, J. A., & Yimam, Z. A. (2022). Spatiotemporal variability and trend analysis of rainfall in Beshilo sub-basin, Upper Blue Nile (Abbaya) Basin of Ethiopia. *Arabian Journal of Geosciences*, 15(16), 1387. <https://doi.org/10.1007/s12517-022-10666-6>
- Mutiibwa, D., Vavrus, S. J., McAfee, S. A., & Albright, T. P. (2015). Recent spatiotemporal patterns in temperature extremes across conterminous United States. *Journal of Geophysical Research: Atmospheres*, 120(15), 7378–7392. <https://doi.org/10.1002/2015JD023598>
- Nash, J. E., & Sutcliffe, J. V. (1970). River flow forecasting through conceptual models part I—A discussion of principles. *Journal of Hydrology*, 10(3), 282–290. [https://doi.org/10.1016/0022-1694\(70\)90255-6](https://doi.org/10.1016/0022-1694(70)90255-6)
- Pendergrass, A. G., Knutti, R., Lehner, F., Deser, C., & Sanderson, B. M. (2017). Precipitation variability increases in a warmer climate. *Scientific Reports*, 7(1), 17966. <https://doi.org/10.1038/s41598-017-17966-y>
- Rossati, A. (2017). Global warming and its health impact. *The international journal of occupational and environmental medicine*, 8(1), 7. <https://doi.org/10.15171/ijocm.2017.963>
- Rossum, G. Van, & Drake, F. L. (2001). *Python reference manual, PythonLabs, Virginia, USA*. Accessed 10 Oct 2021, from <http://www.python.org>
- Setegn, S. G., Srinivasan, R., & Dargahi, B. (2008). Hydrological modelling in the Lake Tana Basin, Ethiopia using SWAT model. *The Open Hydrology Journal*, 2(1), 49–62. <https://doi.org/10.2174/1874378100802010049>
- Teshome, A., & Zhang, J. (2019). Increase of extreme drought over Ethiopia under climate warming. *Advances in Meteorology*, 2019, 1–18. <https://doi.org/10.1155/2019/5235429>
- Uhlenbrook, S., Mohamed, Y., & Gragne, A. S. (2010). Analyzing catchment behavior through catchment modeling in the Gilgel Abay, upper Blue Nile River basin. *Ethiopia. Hydrology and Earth System Sciences*, 14(10), 2153–2165. <https://doi.org/10.5194/hess-14-2153-2010>
- Valencia, S., Marín, D. E., Gómez, D., Hoyos, N., Salazar, J. F., & Villegas, J. C. (2023). Spatio-temporal assessment of Gridded precipitation products across topographic and climatic gradients in Colombia. *Atmospheric Research*, 285(106643), 106643. <https://doi.org/10.1016/j.atmosres.2023.106643>
- Weldegerima, T. M., Zeleke, T. T., Birhanu, B. S., Zaitchik, B. F., & Fetene, Z. A. (2018). Analysis of rainfall trends and its relationship with SST signals in the Lake Tana basin, Ethiopia. *Advances in Meteorology*, 2018, 1–10. <https://doi.org/10.1155/2018/5869010>
- Westra, S., Alexander, L. V., & Zwiers, F. W. (2013). Global increasing trends in annual maximum daily precipitation. *Journal of Climate*, 26(11), 3904–3918. <https://doi.org/10.1175/JCLI-D-12-00502.1>
- Worku, G., Teferi, E., Bantider, A., & Dile, Y. T. (2019). Observed changes in extremes of daily rainfall and temperature in Jemma sub-basin, upper Blue Nile basin,

- Ethiopia. *Theoretical and Applied Climatology*, 135, 839–854. <https://doi.org/10.1007/s00704-018-2412-x>
- Wubaye, G. B., Gashaw, T., Worqlul, A. W., Dile, Y. T., Taye, M. T., Hailelassie, A., & Srinivasan, R. (2023). Trends in rainfall and temperature extremes in Ethiopia: Station and agro-ecological zone levels of analysis. *Atmosphere*, 14(3), 483. <https://doi.org/10.3390/atmos14030483>
- Wubneh, M. A., Kiflelew, M. S., Sahlu, D., Dzwairo, R. B., & Fikadie, F. T. (2022). Hydrological impacts of climate change in selected ungauged sub-watersheds of Lake Tana sub-basin, upper Blue Nile basin, Ethiopia: A regionalization approach. *Scientific African*, 17, e01370. <https://doi.org/10.1016/j.sciaf.2022.e01370>
- Zhang, X., Yang, F., (2004). RCLimDex (1.0) User manual. Climate Research Branch Environment Canada, (p. 22).

**Publisher's Note** Springer Nature remains neutral with regard to jurisdictional claims in published maps and institutional affiliations.

Springer Nature or its licensor (e.g. a society or other partner) holds exclusive rights to this article under a publishing agreement with the author(s) or other rightsholder(s); author self-archiving of the accepted manuscript version of this article is solely governed by the terms of such publishing agreement and applicable law.